Dalton Transactions

COMMUNICATION

View Article Online
View Journal | View Issue

Cite this: *Dalton Trans.*, 2015, **44**, 10928

Received 15th April 2015,
Accepted 5th May 2015

DOI: 10.1039/c5dt01681a

www.rsc.org/dalton

Quantum-CORMs: quantum dot sensitized CO releasing molecules†

A. Ruggi* and F. Zobi*

The synthesis and photodecomposition behaviour of a family of CO releasing molecules (CORMs) based on [Mn(CO)$_3$bpy] derivatives connected to a semiconductor Quantum Dot (QD) sensitizer is described here. Compared to the non-sensitized complexes, such systems show a 2 to 6-fold increase of the photodecomposition rate upon irradiation with visible light.

Since the discovery of the beneficial effects of carbon monoxide (CO) in mammalian physiology, substantial research efforts have been devoted to the development of CO releasing molecules (CORMs) as an alternative for safe and controlled delivery of the gas.[1–7] Most of the CORMs known to date are tailored around transition metal complexes which are able to release CO by thermal activation or hydrolysis in biological media, but controlled and specific CO delivery may also be accomplished by endogenous (*e.g.*, enzymatic reaction)[8–10] or exogenous triggering (*e.g.*, photoexcitation).[11–13] The latter class of molecules, known as photoCORMs (*i.e.* photoactivated CORMs), allows spatial and temporal control over the CO release. Ideally the photoactivation profile of these molecules involves wavelengths in the visible region of the spectrum. This requirement is rarely realized and ultraviolet activation still plays a major role in photoCORMs. A strategy successfully applied to overcome this limitation entails the proper ligand/coligand combination with concomitant extension of the principal ligand conjugation in order to modulate HOMO/LUMO energies and ultimately the MLCT band related to CO photorelease.[14–16] An alternative, yet unexplored, strategy may be the coupling of photoCORMs to semiconductor quantum dots (Fig. 1).

Semiconductor Quantum Dots (QDs) are a class of luminophores showing remarkable performances. Besides a high stability (in the presence of suitable capping units), they usually show luminescence quantum yields often close to unity and a strong molar extinction coefficient at every wavelength smaller than the band-gap. Moreover, their optical and electronic properties can be easily tuned with size during the synthesis.[17,18] For these reasons, QDs have been extensively used for the realization of biological probes, sensitizers in solar cells and high performance optoelectronic devices.[19–22] More recently, QDs have been applied as sensitizers for light-induced release of biologically active molecules like NO and CS_2.[23–26]

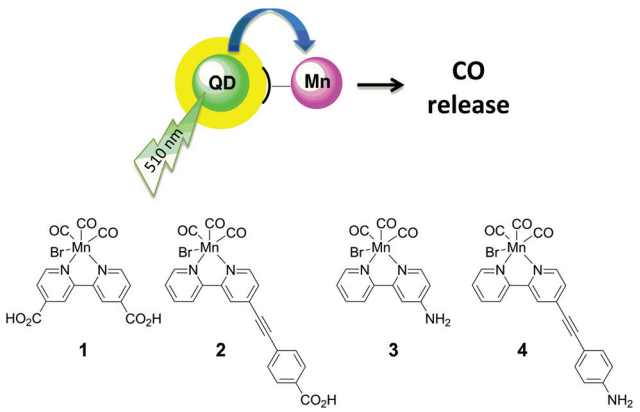

Fig. 1 QD–Mn systems for visible light CO release.

In this communication, we present the first example of QD-sensitized systems capable of releasing CO upon photoirradiation in the visible region of the spectrum. The reported systems are based on *fac*-[Mn(CO)$_3$bpyBr] (bpy = 2,2′-bipyridine) derivatives.[27] Such complexes are known to generate CO upon irradiation in the UV region but show only poor performances at longer wavelengths.[28] In order to improve the CO release rate upon irradiation with visible light, Mn(I) complexes were connected to a QD, thus exploiting the remarkable absorption of semiconductor nanocrystals and their sensitizing capabilities. With the aim of exploring the influence of the QD–Mn distance and of the connecting unit on the sensitization efficiency, we designed a family of complexes in which

Département de Chimie, Université de Fribourg, Chemin du Musée 9, 1700 Fribourg, Switzerland. E-mail: albert.ruggi@unifr.ch, fabio.zobi@unifr.ch

† Electronic supplementary information (ESI) available: Synthetic and analytical details, UV-Vis spectra of Mn(I) complexes and Mn–QD conjugates, and calculation details. See DOI: 10.1039/c5dt01681a

the pristine [Mn(CO)$_3$bpyBr] species is connected to the QD surface either *via* a carboxylic acid (**1**, **2**) or a dithiocarbamate (**3**, **4**).[29] For each connecting unit, a complex bearing a phenylethynyl spacer (**2**, **4**) or no spacer (**1**, **3**) was prepared. The investigation of the photodecomposition behaviour of this family of Mn(I) complexes enabled us to define a general strategy to design QD–Mn systems with improved CO releasing performances upon irradiation with visible light (510 nm).

All complexes were obtained upon reaction of suitable ligands with [Mn(CO)$_5$Br]. Details about the synthesis of the ligands and of the complexes are given in the ESI.† CdSe/ZnS core/shell semiconductor quantum dots having a band-gap wavelength of 504 nm and an emission wavelength of 512 nm were synthesized according to literature procedures.[30] Furthermore, prior to connection with QDs, complexes **3** and **4** were reacted with CS_2, thus converting the amino group into a dithiocarbamate, a functional group known to interact strongly with CdSe/ZnS core/shell quantum dots.[31] Although less explored, carboxylic acids are also capable of binding the ZnS surface. All the QD–Mn systems were obtained by mixing 5 equivalents of each Mn(I) complex to one equivalent of CdSe/ZnS QDs in THF. The resulting mixture was stirred overnight in the dark and then centrifuged to remove the unreacted Mn(I) complexes, exploiting the very poor solubility of the complexes in THF. The modified QDs were then analysed by UV-Vis spectroscopy to estimate the average of Mn(I) connected to every QD (details about the calculation are given in the ESI†). The estimated Mn/QD ratios are 1.7 (**QD-1**), 4 (**QD-2**), 2.5 (**QD-3**) and 3 (**QD-4**). Complexes **1–4** show a bathochromic shift of their absorption bands with respect to the pristine [Mn(CO)$_3$bpyBr] (UV-Vis spectra are given in the ESI†). Upon irradiation at 510 nm, the UV-Vis spectrum of **4** shows a complex behaviour (Fig. 2): the maxima located at 301 nm and 381 nm and the shoulder at 440 nm decrease rapidly with a concomitant emergence of a new band centred at 346 nm. Two isosbestic points (located at 314 and 362 nm) were observed, suggesting the clean transformation of **4**, in agreement with what has been reported in the literature for [Mn(CO)$_3$bpyBr].[28] Conversely, all other complexes only show a decrease of their absorption bands upon photoirradiation. The UV-Vis absorption spectra of the QD–Mn aggregates are an admixture of the absorption spectra of the two components. For instance, in the absorption spectrum of **QD-4**, besides the maximum located at 504 nm (belonging to the QD), two shoulders located at 437 nm and at 383 nm were observed together with a maximum centered at 301 nm (Fig. 2). As expected, these signals are very close to the bands observed for complex **4**. Generally speaking, upon photoirradiation at 510 nm, all the QD–Mn aggregates show a decrease of the high energy bands, whilst the maximum located at 504 nm (band-gap transition of the QD) remains basically unchanged, due to the photostability of the QD. More in detail, in the case of **4** a decrease of the shoulders at 437 nm and 383 nm and the emergence of a new maximum at 343 nm are observed. An isosbestic point is also observed at 360 nm. The similarities observed between the light-induced spectral changes of **QD-4** and the unmodified complex suggest that the same process is taking place, *i.e.* the photodegradation of the Mn(I) species. Evidence of CO release upon irradiation was obtained by performing the myoglobin test (see the ESI†). To evaluate the rate of photodecomposition, a kinetic analysis was performed recording the UV-Vis spectra after different irradiation times (Fig. 3). Upon irradiation at 510 nm, all species show a first order photodegradation kinetic, although with different rate constants and half-lives. Kinetic data are given in Table 1. Generally speaking, complexes **1–4** show shorter decomposition half-lives $t_{1/2}$ (*i.e.* a faster photodecomposition) with respect to the pristine [Mn(CO)$_3$bpyBr] complex. This effect corresponds to an augmentation of the decomposition constant k_{dec} up to a factor of 6 and is likely due to the higher absorption shown by the studied complexes in the excitation region (510 nm). More interestingly, upon connection with QDs, the complexes show a further decrease of their decomposition half-lives. The complexes bearing no spacers (*i.e.* **1** and **3**) show the most prominent acceleration of their decomposition kinetics: upon connection with the QD, the decomposition half-life is decreased by a factor of 2, in the case of **1**, and by a factor of 6, in the case of **3**. These values are in line with the results reported by Ford *et al.* concerning NO-sensitized emission of

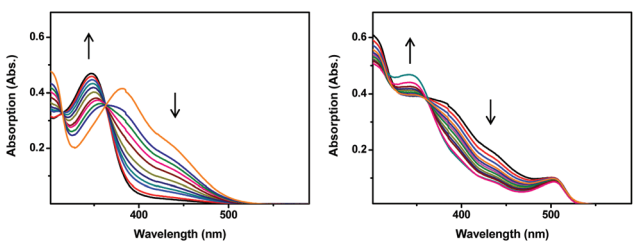

Fig. 2 Changes in the UV-Vis spectrum upon irradiation at 510 nm of **4** (left) and **QD-4** (right). Equimolar solutions in THF (5% MeOH).

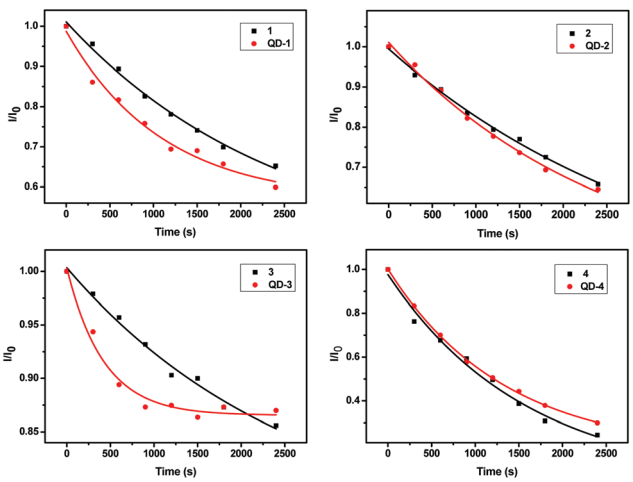

Fig. 3 Kinetics of photodegradation upon irradiation at 510 nm. Equimolar solutions in THF (5% MeOH).

Table 1 Kinetic and photochemical data of complexes and their conjugation with QD

	$\langle\tau\rangle^a$ (ns)	$k_q{}^b/10^7$ (s^{-1})	$J/10^{13}$ ($nm^4\ M^{-1}\ cm^{-1}$)	$k_{dec}/10^{-4}$ (s^{-1})	$t_{1/2}{}^c$ (s)
$[Mn(CO)_3bpyBr]$	—	—	—	1.0 ± 0.2	6931
1	—	—	—	5.2 ± 0.7	1333
2	—	—	—	2.2 ± 0.2	3151
3	—	—	—	3.9 ± 1.0	1777
4	—	—	—	5.9 ± 0.9	1175
QD	17.1	—	—	—	—
QD-1	9.6	2.7	4.3	10.0 ± 0.1	693
QD-2	9.6	1.1	6.4	4.1 ± 0.3	1733
QD-3	11.8	1.1	15.3	24.1 ± 0.4	288
QD-4	10.5	1.2	6.5	6.5 ± 0.2	1066

$^a\langle\tau\rangle$ = average lifetime. $^b k_q$ = normalised quenching constant. $^c t_{1/2}$ = decomposition half-life.

non-optimised systems based on QDs.[23,25] A 2-fold half-life decrease is also observed for complex **2**, bearing a 0.5 nm spacer, whilst complex **4** shows negligible decrease. The calculated kinetic constants and half-lives are summarized in Table 1. Since first order kinetics do not depend on the initial concentration of the reagent (*i.e.* on the different amounts of Mn(I) complexes connected to the QD), the observed differences are attributable to a different sensitization efficiency. To obtain more information concerning the processes taking place in the systems, the quenching of QD luminescence was studied with time-resolved fluorimetry. The results of these investigations are summarised in Table 1. A multicomponent decay is typically observed for QDs.[23] In fact, in our samples all decays can be fitted with a three components exponential equation. All the conjugated systems show a pronounced quenching: the quenching constants k_q normalised taking into account the number of Mn(I) complexes present on the QD (see the ESI†) are equal to $2.7 \times 10^7\ s^{-1}$ and $1.1 \times 10^7\ s^{-1}$ for **QD-1** and **QD-2** respectively.[24] Conversely, the normalised quenching constants calculated for **QD-3** and **QD-4** are equal to $1.1 \times 10^7\ s^{-1}$ and $1.2 \times 10^7\ s^{-1}$ respectively. To obtain a preliminary evaluation of the quenching mechanism (namely energy or electron transfer), the Mn(I) complex absorption/QD emission overlapping integral (J) was calculated (see the ESI†). In the case of the pair **QD-1**/**QD-2**, the trend of the quenching constant is not connected to the value of J (which actually increases passing from **QD-1** to **QD-2**). However, the observed k_q trend is qualitatively in line with the expected reduction of both energy and electron transfer efficiency induced by the introduction of a 0.5 nm spacer in **QD-2** with respect to **QD-1**.[32] The changes observed in the photodecomposition kinetic constants are proportional to the variations observed in the quenching constant. However, on the basis of the available data, it is not possible to discriminate between the two processes, which could both be efficient for Mn(I) sensitization.[33] In the case of the pair **QD-3**/**QD-4**, basically the same k_q is observed, in spite of the introduction of the spacer and the decrease of J passing from **QD-3** to **QD-4**. We have interpreted these surprising results in terms of an energy or electron transfer taking place between the QD and the dithiocarbamate moiety of the complex. Such hypothesis is corroborated by previous studies, in which an emission quenching, due to a charge transfer, was observed in CdSe QDs functionalised with aromatic moieties bearing dithiocarbamate groups.[34] In the case of **QD-3** and **QD-4** the observed variation of photodecomposition constant is not related to the quenching constant. This would suggest the presence of another process (*e.g.* a two-step energy or electron transfer) taking place in such systems and not accessible to time-resolved fluorimetry. Further studies involving transient absorption spectroscopy are currently ongoing, aimed at a complete elucidation of the sensitization mechanism.

Conclusions

In conclusion, we have reported here the first examples of QD-sensitized CO releasing systems based on a CdSe/ZnS core/shell quantum dot connected to Mn(I) complexes. Compared to non-sensitized complexes, such systems show a 2 to 6-fold increase of their photodecomposition rate upon irradiation at 510 nm. The reported systems constitute a proof of principle of the possibility of exploiting the remarkable optical properties of semiconductor QDs to improve the CO releasing rate of CORMs. We are currently studying the sensitization mechanism in order to design new systems with optimised properties and higher CO releasing efficiency.

Acknowledgements

The authors thank Felix Fehr for support with NMR spectroscopy. F. Z. thanks SNSF (grant PP00P2_144700) for funding.

Notes and references

1 R. Motterlini and L. E. Otterbein, *Nat. Rev. Drug Discovery*, 2010, **9**, 728–743.
2 F. Zobi, *Future Med. Chem.*, 2013, **5**, 175–188.
3 B. E. Mann, in *Medicinal Organometallic Chemistry*, ed. G. Jaouen and N. Metzler Nolte, 2010, vol. 32, pp. 247–285.
4 U. Schatzschneider, *Br. J. Pharmacol.*, 2015, **172**, 1638–1650.
5 C. C. Romao, W. A. Blaettler, J. D. Seixas and G. J. L. Bernardes, *Chem. Soc. Rev.*, 2012, **41**, 3571–3583.
6 S. H. Heinemann, T. Hoshi, M. Westerhausen and A. Schiller, *Chem. Commun.*, 2014, **50**, 3644–3660.
7 S. Garcia-Gallego and G. J. L. Bernardes, *Angew. Chem., Int. Ed.*, 2014, **53**, 9712–9721.
8 S. Romanski, B. Kraus, U. Schatzschneider, J.-M. Neudoerfl, S. Amslinger and H.-G. Schmalz, *Angew. Chem., Int. Ed.*, 2011, **50**, 2392–2396.

9 S. Romanski, H. Ruecker, E. Stamellou, M. Guttentag, J.-M. Neudoerfl, R. Alberto, S. Amslinger, B. Yard and H.-G. Schmalz, *Organometallics*, 2012, **31**, 5800–5809.
10 E. Stamellou, D. Storz, S. Botov, E. Ntasis, J. Wedel, S. Sollazzo, B. K. Kramer, W. van Son, M. Seelen, H. G. Schmalz, A. Schmidt, M. Hafner and B. A. Yard, *Redox Biol.*, 2014, **2**, 739–748.
11 R. D. Rimmer, A. E. Pierri and P. C. Ford, *Coord. Chem. Rev.*, 2012, **256**, 1509–1519.
12 J. S. Ward, J. M. Lynam, J. Moir and I. J. S. Fairlamb, *Chem. – Eur. J.*, 2014, **20**, 15061–15068.
13 J. S. Ward, J. M. Lynam, J. W. B. Moir, D. E. Sanin, A. P. Mountford and I. J. S. Fairlamb, *Dalton Trans.*, 2012, **41**, 10514–10517.
14 S. J. Carrington, I. Chakraborty, J. M. L. Bernard and P. K. Mascharak, *ACS Med. Chem. Lett.*, 2014, **5**, 1324–1328.
15 S. J. Carrington, I. Chakraborty and P. K. Mascharak, *Chem. Commun.*, 2013, **49**, 11254–11256.
16 I. Chakraborty, S. J. Carrington and P. K. Mascharak, *Acc. Chem. Res.*, 2014, **47**, 2603–2611.
17 B. O. Dabbousi, J. RodriguezViejo, F. V. Mikulec, J. R. Heine, H. Mattoussi, R. Ober, K. F. Jensen and M. G. Bawendi, *J. Phys. Chem. B*, 1997, **101**, 9463–9475.
18 P. Reiss, M. Protiere and L. Li, *Small*, 2009, **5**, 154–168.
19 K. Mukai, *J. Nanosci. Nanotechnol.*, 2014, **14**, 2148–2156.
20 M. F. Frasco and N. Chaniotakis, *Sensors*, 2009, **9**, 7266–7286.
21 B. A. Kairdolf, A. M. Smith, T. H. Stokes, M. D. Wang, A. N. Young and S. Nie, *Annu. Rev. Phys. Chem.*, 2013, **6**, 143–162.
22 P. V. Kamat, *J. Phys. Chem. C*, 2008, **112**, 18737–18753.
23 D. Neuman, A. D. Ostrowski, A. A. Mikhailovsky, R. O. Absalonson, G. F. Strouse and P. C. Ford, *J. Am. Chem. Soc.*, 2008, **130**, 168–175.
24 P. T. Burks, A. D. Ostrowski, A. A. Mikhailovsky, E. M. Chan, P. S. Wagenknecht and P. C. Ford, *J. Am. Chem. Soc.*, 2012, **134**, 13266–13275.
25 D. Neuman, A. D. Ostrowski, R. O. Absalonson, G. F. Strouse and P. C. Ford, *J. Am. Chem. Soc.*, 2007, **129**, 4146–4147.
26 C. M. Bernt, P. T. Burks, A. W. DeMartino, A. E. Pierri, E. S. Levy, D. F. Zigler and P. C. Ford, *J. Am. Chem. Soc.*, 2014, **136**, 2192–2195.
27 R. A. Motterlini, B. E. Mann and D. A. Scapens, *Patent WO* 2008/003953, 2008.
28 G. J. Stor, S. L. Morrison, D. J. Stufkens and A. Oskam, *Organometallics*, 1994, **13**, 2641–2650.
29 M. Green, *J. Mater. Chem.*, 2010, **20**, 5797–5809.
30 S. Impellizzeri, S. Monaco, I. Yildiz, M. Amelia, A. Credi and F. M. Raymo, *J. Phys. Chem. C*, 2010, **114**, 7007–7013.
31 F. Dubois, B. Mahler, B. Dubertret, E. Doris and C. Mioskowski, *J. Am. Chem. Soc.*, 2007, **129**, 482–483.
32 J. R. Lackowicz, *Principles of Fluorescence Spectroscopy*, Springer, Singapore, 2006.
33 P. T. Burks and P. C. Ford, *Dalton Trans.*, 2012, **41**, 13030–13042.
34 Y. Tan, S. Jin and R. J. Hamers, *ACS Appl. Mater. Interfaces*, 2013, **5**, 12975–12983.